Supplementary Information

Indole-Based Conjugated Macromolecule as Redox-Mediated Electrolyte for Ultrahigh Power Supercapacitor

Ting Xiong [a,b,⊥], Wee Siang Vincent Lee [a,⊥], Li Chen [c], Teck Leong Tan[d], Xiaolei Huang [*a], Junmin Xue[*] [a]

[a] National University of Singapore, Department of Materials Science and Engineering, Singapore 117573.

[b] Centre for Advanced 2D Materials and Graphene Research Centre, National University of Singapore, Singapore 117546.

[c] Department of Chemistry, Tianjin University, Tianjin 300072, People's Republic of China

[d] Institute of High Performance Computing, A*STAR, 1 Fusionopolis Way, #16-16 Connexis, Singapore 138632

[*]To whom correspondence should be addressed. E-mail: msexuejm@nus.edu.sg (Junmin Xue), msehx@nus.edu.sg (Xiaolei Huang), Tel./fax +65 65164655.

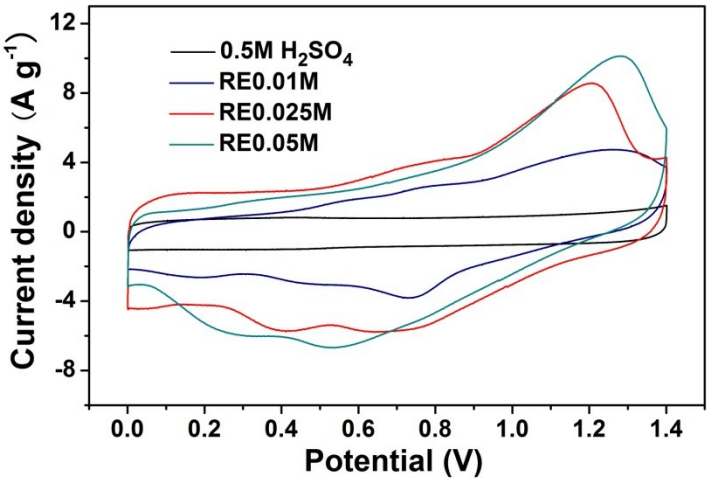

Fig. S1 CV curves of the obtained porous honeycomb-like carbon using dopamine with different concentration as the redox-active additive at scan rate of 25 mV s^{-1}.

Inspired by this, we firstly studied dopamine as a redox additive in supercapacitor. By using the prepared porous honeycomb-like carbon (labeled as PHC) as the electrode material, we tested the capacitive performance of the redox-active electrolyte using a two-electrode configuration. As shown in Fig. S1, PHC showed excellent rectangle-like cyclic voltammetry curves in 0.5 M H_2SO_4 in the potential range of 0 – 1.4 V. The addition of dopamine into 0.5 M H_2SO_4 solution caused increases in capacitance, and the capacitance increased gradually with the concentration of dopamine from 0.01 M to 0.05 M (certain amount of dopamine chloride was dissolved into 50 mL of 0.5 M H_2SO_4 to obtain 0.01 mol L^{-1} (M), 0.025 M, and 0.05 M dopamine solution, which were labeled as RE0.01M, RE0.025M and RE0.05M, respectively). Notably, strong peaks related to the redox reaction of phenolic hydroxyl group/quinoid carbonyl group (equation (1)) were observed, which contributed to the pseudocapacitance. Among the three redox electrolytes, the cyclic voltammetry curves of the porous honeycomb-like carbon in RE0.025M electrolyte was much rectangle-like, suggesting that the optimal concentration of dopamine was 0.025M.

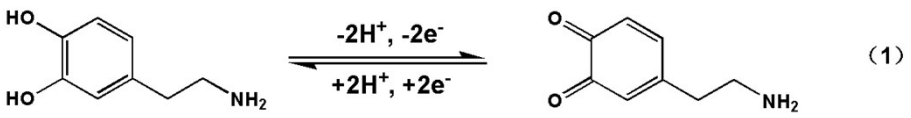

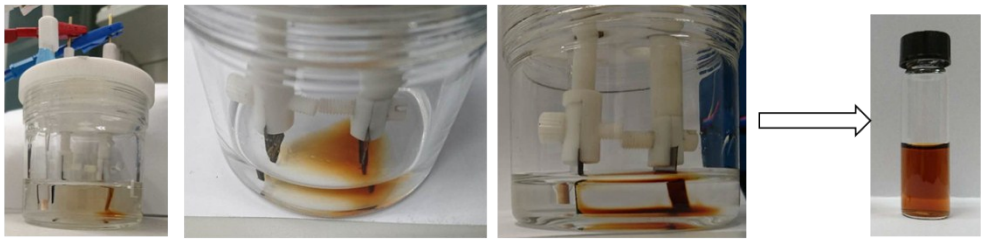

Fig. S2 The transformation process of RE0.025M to BRE0.025M in the three electrode at scan rate of 1000 mV s^{-1}.

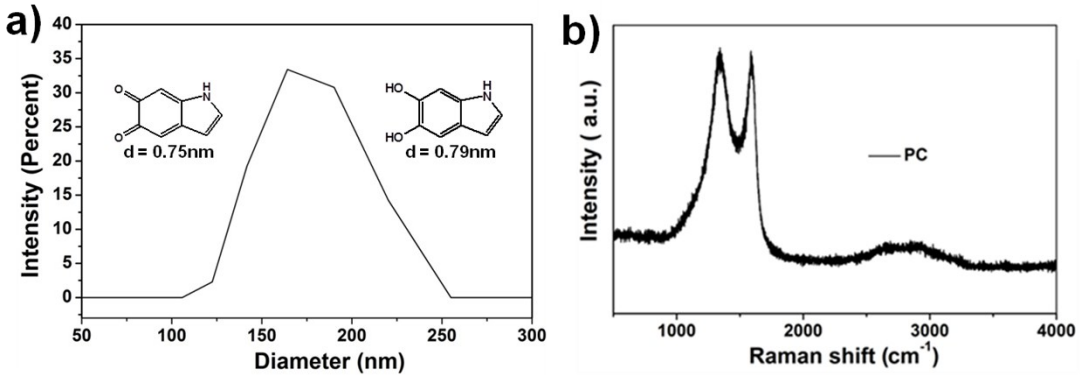

Fig. S3 a) The size distribution of the molecules in BRE0.025M electrolytes; b) The Raman spectrum of PC.

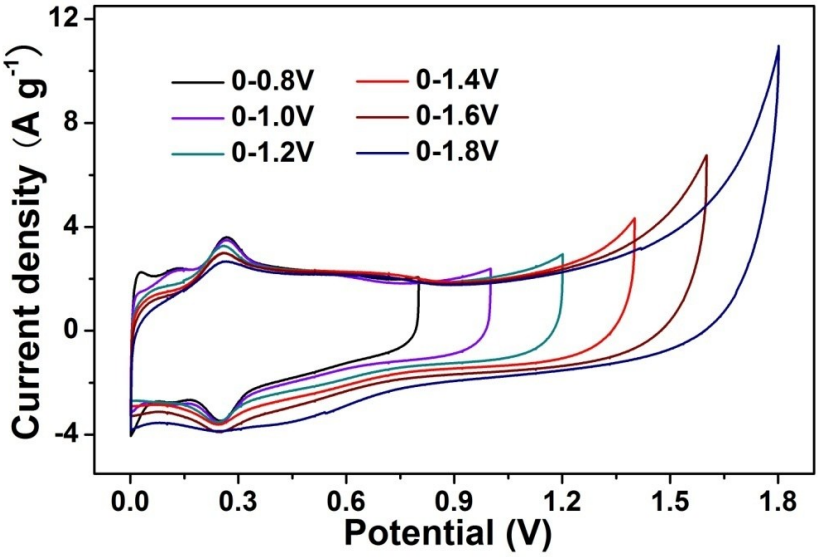

Fig. S4 The cyclic voltammetry (CV) curves of the porous honeycomb-like carbon with step-wise potential increment of 0.2 V from an initial potential window of 0.8 V to a final potential window of 1.8V in BRE0.025M electrolyte at scan rate of 25 mV s^{-1}.

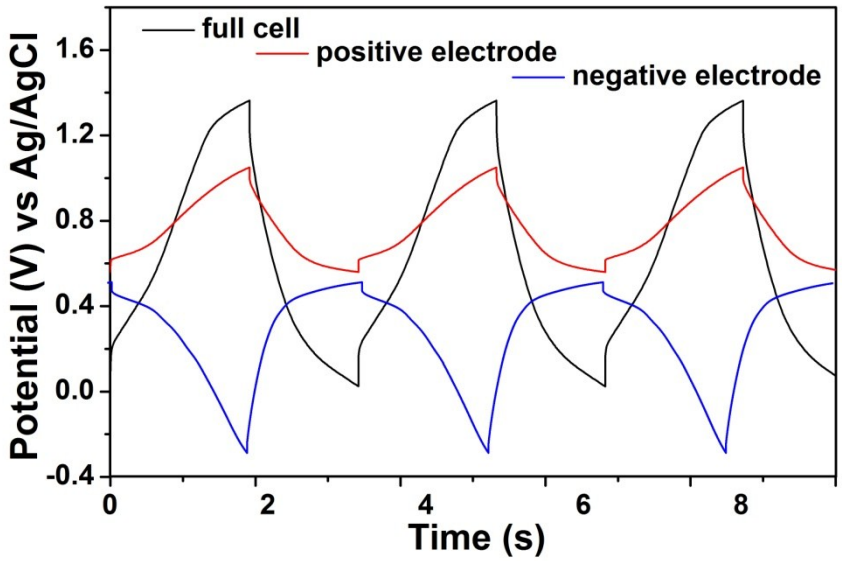

Fig. S5 Three electrodes test to investigate the individual contribution of negative and positive electrodes in the BRE0.025M electrolyte.

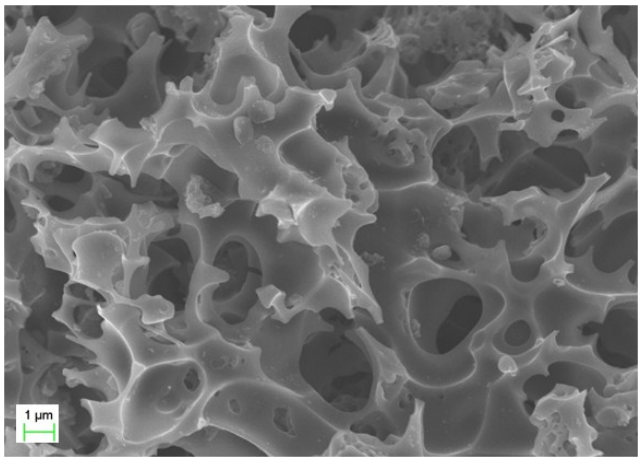

Fig. S6 SEM image of PC.

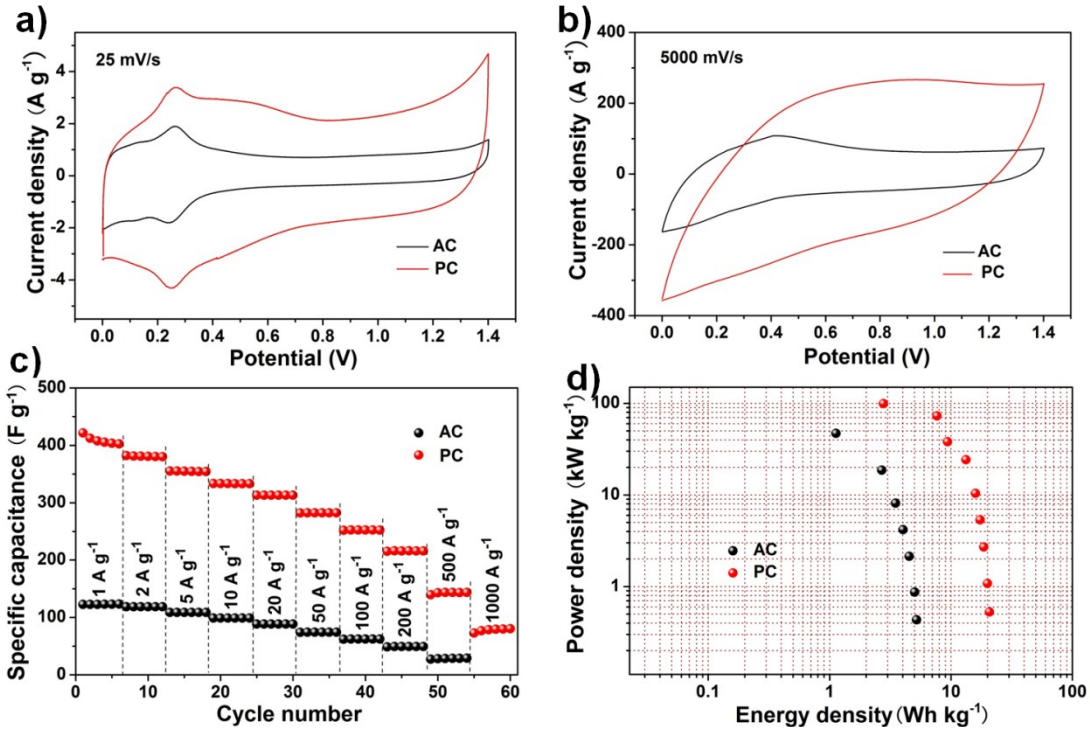

Fig. S7 Electrochemical characterization of AC and PC using BRE0.025M electrolyte. (a),(b), CV curves; (c) rate performance at different current densities; (d) Ragone plot.

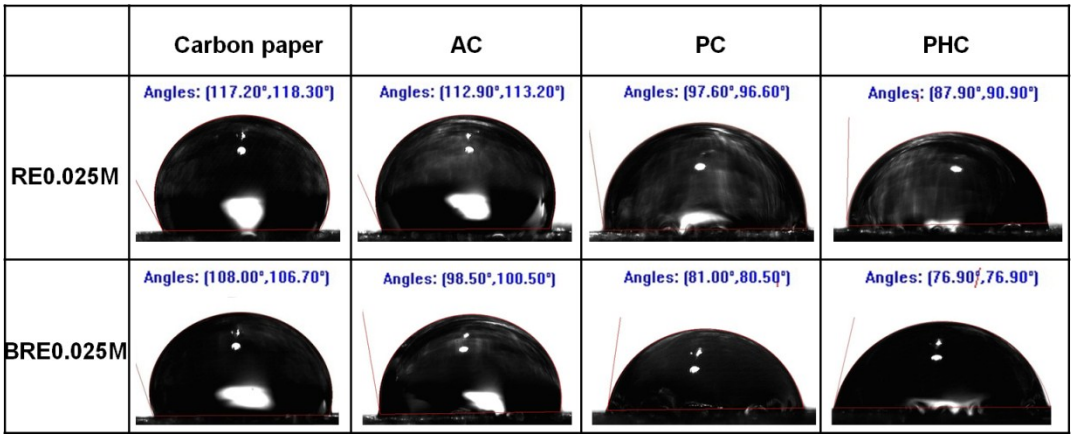

Fig. S8 Dynamic electrolyte contact angle measurements for the bare carbon paper, porous honeycomb-like carbon (PHC), activated carbon (AC) and another porous carbon (PC) in the RE0.025M and BRE0.025M electrolytes.

Table S1. Comparison of the supercapacitor performance parameters for redox supercapacitors and our present work.

Active material	Electrolytes	Potential window	Capacitance	Max Energy density	Max Power density	Capacitance retention	Ref.
Activated carbon	$Fe(CN)_6^{3-}$/ $Fe(CN)_6^{4-}$ in 1M Na_2SO_4	0–2 V	364.6 mF cm^{-2}	18.9 Wh kg^{-1}	11.5 kW kg^{-1}	80% after 7000 cycles	1
Activated carbon (KOH activated)	0.38 M Hydroquinone in 1 M H_2SO_4	0–1 V	901 Fg^{-1}	18 Wh kg^{1}	12 kW kg^{-1}	65%after 4000 cycle	2
N/O-functionalized nanoporous carbon	Pyrocatechol in 1 M H_2SO_4	0–1 V	368.7 F g^{-1}	124.4 Wh kg^{-1}	29.9 kW kg^{-1}	96.4% after 5000 cycles	3
carbon/1, 4-dihydroxyanthraquinone	Hydroquinone in 1M H_2SO_4	0–1 V	239 F g^{-1}	21.1 Wh kg^{-1}	5.0 kW kg^{-1}	91.6 % after 5000 cycles	4
carbon nanosheets	Anthraquinone-2-sulfonic acid sodium and KI in 1M KNO_3	0–1.8 V	75 F g^{-1}	33.8 Wh kg^{-1}	10 kW kg^{-1}	95.2 % after 5000 cycles	5
Hierarchical α-MnO_2 tube-on-tube arrays	1.0 M Na_2SO_4	0–0.8 V	213 F g^{-1}	20.8 Wh kg^{-1}	3.2 kW kg^{-1}	—	6
phosphate ion functionalized Co_3O_4	6.0 M KOH	0–1.5 V	229 F g^{-1}	71.58 Wh kg^{-1}	24 kW kg^{-1}	95% after 2000 cycles	7
Mn_3O_4 embedded on carbon	1 M Na_2SO_4	0–0.8 V	195 F g^{-1}	4.3 Wh kg^{-1}	52 kW kg^{-1}	59% after 60h	8
$Fe(CN)_6^{3-}$ modified Carbon	1 M Na_2SO_4	0–1.8 V	15 W h kg^{-1} —	15 W h kg^{-1} 15 Wh kg^{-1}	79.1 kW kg^{1}	100% after 20000 cycles	9
Porous honeycomb-like carbon	indole-based conjugated macromolecular in 0.5 M H_2SO_4	0–1.4 V	550 F g^{-1}	31.6 Wh kg^{-1}	153 kW kg^{-1}	97.1% after 20000 cycles	this work

Table S2. Comparison of the supercapacitor performance parameters for EDLC supercapacitors and our present work.

Active material	Electrolytes	Potential window	Capacitance	Max Energy density	Max Power density	Capacitance retention	Ref.
3D porous RGO films	1.0 M H_2SO_4	0–1 V	284.2 F g^{-1}	9.9 Wh kg^{-1}	282 kW kg^{-1}	97.6% after 10000 cycles	10
3D Few-Layer Graphene-like Carbon	6 M KOH	0–1 V	219 F g^{-1}	8 Wh kg^{-1}	199.7 kW kg^{-1}	99% after 20000 cycles	11
porous carbon foam electrode with multiscale pore network	LiOH-PVA	0–1 V	315.2 F g^{-1}	10.4 Wh kg^{-1}	250 kW kg^{-1}	97.6 % after 10000 cycles	12
Nitrogen-doped mesoporous carbon	0.5 M H_2SO_4	0–1.2 V	855 F g^{-1}	39.5 Wh kg^{-1}	42.5 kW kg^{-1}	82 % after 50000 cycles	13
N-Doped carbon nanocages	6 M KOH	0–1 V	313 F g^{-1}	10.9 Wh k^{-1}	22.2 kW kg^{-1}	98% after 50000 cycles	14
Graphene films	6 M KOH	0–1 V	178 F g^{-1}	~6 Wh kg^{1}	112.6 kW kg^{-1}	95 % after 2000 cycles	15
Porous honeycomb-like carbon	indole-based conjugated macromolecular in 0.5 M H_2SO_4	0–1.4 V	550 F g^{-1}	31.6 Wh kg^{1}	153 kW kg^{-1}	97.1% after 20000 cycles	this work

References

1 J. Y. Hwang, M. Li, M. F. El-Kady and R. B. Kaner, *Adv. Funct. Mater*., 2017, **27**, 1605745.
2 S. Roldán, C. Blanco, M. Granda, R. Menéndez and R. Santamaría, *Angew. Chem. Int. Ed*., 2011, **50**, 1699–1701.
3 Y. F. Nie, Q. Wang, X. Y. Chen and Z. J. Zhang, *J. Power Sources*, 2016, **320**, 140–152.
4 D. Xu, X. N. Sun, W. Hu and X. Y. Chen, *J. Power Sources*, 2017, **357**, 107–116.
5 X. N. Sun, D. Xu, W. Hu and X. Y. Chen, *ACS Sustainable Chem. Eng*., 2017, **5**, 5972–5981.
6 B. Z. Yu, X. D. Zhao, J. Luo, H. G. Zhang, Y. W. Zhu, G. Y. Jing, P. Ma, Z. Y. Ren and H. M. Fan, *Adv. Mater. Interfaces*, 2016, **3**, 1500761.
7 T. Zhai, L. Wan, S. Sun, Q. Chen, J. Sun, Q. Xia and H. Xia, *Adv. Mater.*, 2017, **29**, 1604167.
8 K. Makgopa, K. Raju, P. M. Ejikeme and K. I. Ozoemena, *Carbon*, 2017, **117**, 20–32.
9 L. Sheng, L. Jiang, T. Wei, Z. Liu and Z. Fan, *Adv. Energy Mater*., 2017, 1700668.
10 Y. Shao, M. F. El-Kady, C.-W. Lin, G. Zhu, K. L. Marsh, J. Y. Hwang, Q. Zhang, Y. Li, H. Wang and R. B. Kaner, *Adv. Mater*., 2016, **28**, 6719–6726.
11 J. Zhao, Y. Jiang, H. Fan, M. Liu, O. Zhuo, X. Wang, Q. Wu, L. Yang, Y. Ma and Z. Hu, *Adv. Mater*., 2017, **29**, 1604569.
12 F. Zhang, T. Liu, M. Li, M. Yu, Y. Luo, Y. Tong and Y. Li, *Nano Lett*., 2017, **17**, 3097−3104.
13 T. Lin, I.-W. Chen, F. Liu, C. Yang, H. Bi, F. Xu and F. Huang, *Science*, 2015, **350**, 1508−1513.
14 J. Zhao, H. Lai, Z. Lyu, Y. Jiang, K. Xie, X. Wang, Q. Wu, L. Yang, Z. Jin, Y. Ma, J. Liu and Z. Hu, *Adv. Mater*., 2015, **27**, 3541−3545.
15 Z. Bo, W. Zhu, W. Ma, Z. Wen, X. Shuai, J. Chen, J. Yan, Z. Wang, K. Cen, X. Feng, *Adv. Mater*., 2013, **25**, 5799−5806.